Site controlled Red-Yellow-Green light emitting InGaN Quantum Disks on nano-tipped GaN rods

M. Conroy[†‡§‖*], *H. Li*[†‡], *G. Kusch*[¶], *C. Zhao*[ǂ], *B. Ooi*[ǂ], *R. W. Martin*[¶], *J. D. Holmes*[†§‖], *P. J. Parbrook*[†‡*]

[†] Tyndall National Institute, Dyke Parade, Cork City, Ireland

[‡] School of Engineering, University College Cork, Cork City, Ireland

[§] Department of Chemistry, University College Cork, Cork City, Ireland

[‖] AMBER@CRANN, Trinity College Dublin, Dublin City, Ireland

[¶] Department of Physics, SUPA, University of Strathclyde, 107 Rottenrow, Glasgow G4 0NG, U.K.

[ǂ] Photonics Laboratory, King Abdullah University of Science and Technology (KAUST), Thuwal 23955-6900, Saudi Arabia

KEYWORDS

Nitrides, nanorods, STEM, EDX, MOCVD, InGaN

ABSTRACT

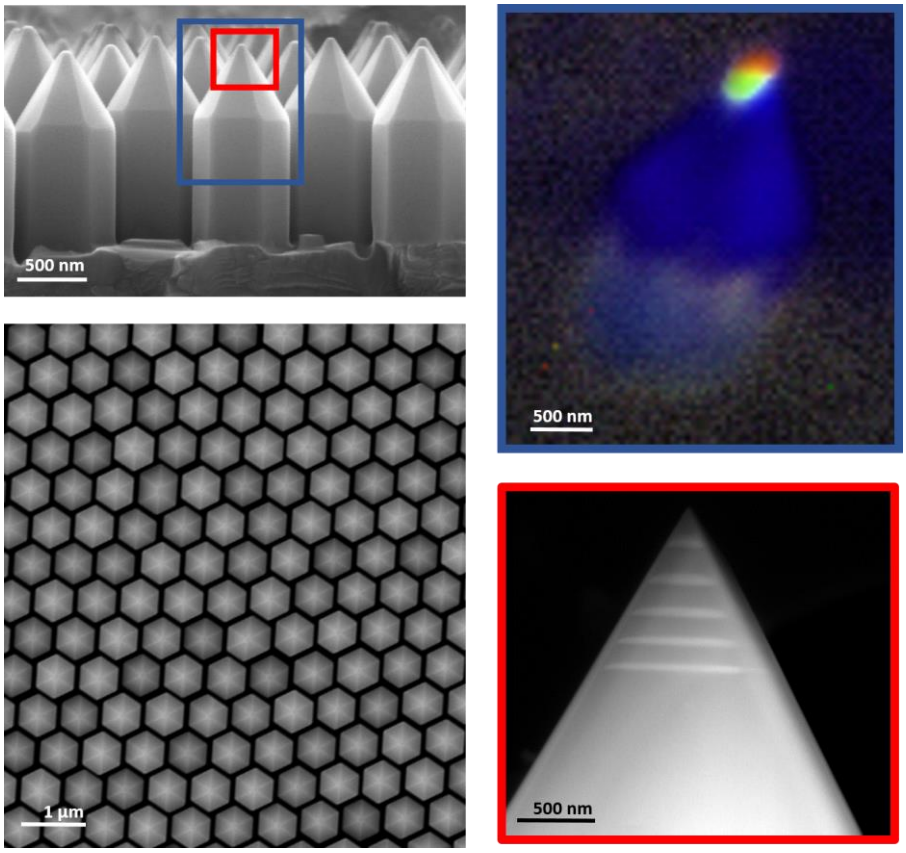

InGaN/GaN multiple quantum well (MQW) hetero-structures grown by metal organic chemical vapour deposition (MOCVD) on the ultra-high density >80% space filling GaN nanororod templates is reported for the first time. The nanorod tips have broad emission in the red yellow and green (RYG) visible range by manipulating the InGaN nano-disks' confinement dimensions along the top of the nanorod. Correlative scanning transmission electron microscopy (STEM) energy-dispersive x-ray (EDX) mapping and hyperspectral cathodoluminescence (CL) imaging illustrates the controlled site selection of the RYG emission at these tips. The 200 nm red emission shift from the active region at the base of the nanorod to the top indicates that the quantum confined stark effect, induced by the natural piezoelectric polarization along the polar facet of GaN, is enhanced by the increasing InGaN MQW thickness. While strain relaxation of the nano-scale dimensions at

the sharp tipped nanorods and dislocation free structure allow for the increased radiative recombination within these thick InGaN MQWs not seen in the highly strained InGaN MQWs grown on bulk layers.

INTRODUCTION

InGaN based semiconductor optoelectronic devices are leading the way in the evolution of broad spectrum solid state lighting.[1-4] Their potential wavelength emission can in theory produce light across the entire visible spectrum simply by alloying In% in the InGaN active region.[5] Although light emitting diodes (LEDs) promise a high degree of functionality and performance, there are still improvements required to reach the longer wavelengths beyond blue emission. Growing InGaN MQWs with sufficient In% to emit light above 520 nm has been difficult due to the crystallographic defects formed, better known as the "green gap".[6] As InGaN grown on GaN increases in thickness there is a huge stress caused by the lattice mismatch.[7] The main stress relieving mechanisms possible for epitaxially grown InGaN on planar layers is through dislocation formation[8-9] which are known to have a significant impact on the internal quantum efficiency.[10] GaN nanorods used as the template for InGaN MQW growth provide a strain free surface without dislocations due to the large surface-to-volume ratio of III-N nanorods.[11-13] These dislocation free GaN nanostructures are also reported to increase light extraction efficiency and enlarge the light emitting surface.[14-16] Additionally moving from bulk to nanoscale provides many new optical properties[17-18] bridging the green gap.

Until recently GaN nanorods were mainly produced by bottom up growth methods such as spontaneous self-assembly molecular beam epitaxy[19], vapor liquid solid[20-21] and selective area

growth.[10] Although these methods can produce high crystal quality GaN with negligible extended defect content, their spontaneous origin causes increasingly large areas of coalescence to be formed with increasing density.[22] At these coalesced nanorod regions the mutual misorientation results in extended defects such as basal plane stacking faults and dislocations when the strain cannot be accommodated elastically.[23-25] The increased strain caused by the coalescence has a significant impact on the optical properties of the nanorod LEDs: as reported by several groups the PL peaks broaden greatly with increasing fill factor.[19, 26-28] Furthermore, additional peaks associated with basal stacking faults[25, 29] and threading dislocations[30] only begin to appear above a certain fill factor. To overcome these issues a new two-step top down/bottom up method has started to be used for high crystal quality GaN nanorods.[31-35] This allows for the combined benefits from planar crystal growth such as low impurity incorporation and controlled doping; and nanorod architecture benefits such as low dislocation density and strain. This two-step method avoids coalescence by spacing out the nanorods in an organized pattern thus lowering the density of rods significantly. However high fill factor/density is an essential aspect for GaN nanorod LEDs to decrease the required current density in the junction at constant total currents.[36] Using a modified space filling growth model as we reported previously for AlN elsewhere,[37] InGaN active regions can now be grown on highly dense (>80%) arrays avoiding the issue of coalescing rods.

In this letter we measure by hyperspectral CL a red shift of >100 nm at the c-plane nanotips, showing five distinct emission peaks from 514-635 nm/RYG. The growth parameters of the InGaN MQWs such as growth rate,[38-39] time[40-41] and temperature[42-43] are traditionally manipulated to increase the indium content and consequently increase the emission wavelength. However this increasing indium content and/or thick MQWs results in poor crystal quality layers mostly due to the large lattice mismatch and difference in thermal expansion coefficients with the GaN barriers[44],

forming centres or non-radiative recombination. For our study the growth parameters were kept constant for all five MQWs with a low indium content of ~15%. The red shift in fact appears to be achieved by simply manipulating the confinement dimensions of the active regions at the top of 3D structure nanorods. We show by STEM physical characterization of the InGaN MQWs, the inverse linear relationship between the QW thicknesses in the x/y directions to the z direction (0001 growth direction) at the top of the truncated pyramidal GaN nanorods. This greatly increased growth rate occurring selectively at the rod top c-planes, allows for the site controlled RYG emission only at the nanotips.

Initially GaN bulk layers (typically 2 μm thick) were grown by MOCVD using an Aixtron close coupled showerhead 3 x 2" reactor on top of our AlN/Al_2O_3 templates.[45] Using the same silica sphere monolayer self-assembly method as in our previous report for AlN nanorods[46-47] a close packed nano dimensional hard mask was coated over the entire 2" wafer, as seen in the photograph of Figure 1e. The close packed silica sphere hard mask (SSHM) was spaced out using an inductively coupled plasma (ICP) CF_4 based etch that selectively etched/shrunk the silica spheres without affecting the GaN bulk layer, schematically represented in Figure 1a and b. The spaced-out pattern was then transferred into the GaN using a 2.5 min Cl_2 based ICP etch to form ~1.75 μm long nanorods, as seen in the illustration and scanning electron micrograph (SEM) of Figure 1c. An estimated 300 nm of GaN was overgrown on nanorod patterns (estimated by in-situ growth reflectance measurements carried out using a Laytec EpiTT system on a planar GaN wafer) at a growth temperature of 900 °C and V/III ratio of 2400 by MOCVD. The SEM imaging of the resulting overgrowth surface as seen below the schematic illustration in Figure 1d, reveals the highly dense semi-polar sided pyramidal topped GaN nanorods without coalescence. To overcome the parasitic growth and coalescing between the GaN rods, the originally etch depth was increased

to a depth longer than the estimated diffusion length of the Ga adatom species under these growth parameters. Hence any GaN deposition/growth at points further down the nanorod can only occur due to the direct impingement of the incoming flux. GaN overgrowth on nanorod patterns etched for a shorter etch time of 1 min (etch depth of ~700 nm) resulted in the coalesced regions between adjacent rods as expected, Figure S1 of supporting information. Therefore after a certain nanorod etch depth there will be no GaN growth, keeping the adjacent nanrod bases separate and avoiding any parasitic growth between the bases of the rods.

The naturally occurring hexagonal alignment of the top-down etched nanorod pattern resulted in a non-polar sidewall meeting point of the grown nanorods. The stability of these non-polar facets inhibited the coalescence of the rods at these meeting points under the growth conditions used, hence an ultra-dense array of space filling nanorods was easily achieved even at high temperature of 900 ^{0}C. Due to the randomness of the GaN nanorods positioning when growth is done using spontaneous growth modes[22], coalescence occurs easily and the highest space filling factor without coalescence achieved to date is only 50%.[36] The issue of coalescing is only seen for our approach when the pattern of the original silica sphere hard mask was not well aligned. Although there are many benefits to self-assembly patterning, long ranged order is only achievable to a certain extent. When the grain boundaries of two crystallites meet the change in the ordering can result in a "perfect misalignment", where one of the adjacent nanorods is twisted by 30$^{\mathbf{o}}$ to the neighboring rod. These misaligned nanorods coalesce causing the vertical growth rate to increase at these points as seen in supporting information Figure S2. However, with increasing growth deposition (300 nm → 1 μm) the majority of the nanorods remain stand-alone it is still only at the "perfectly misaligned" points that coalescence occurs.

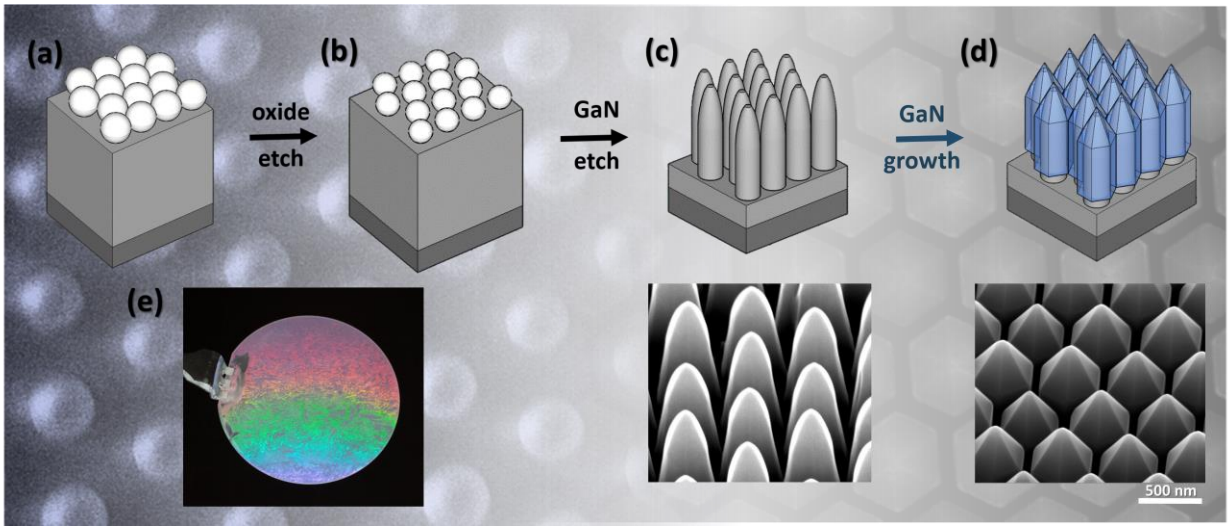

Figure 1 Schematic illustration of the processing and growth steps of the GaN nanorod formation (a) close packed monolayer of silica spheres on GaN bulk layer, (b) spaced out monolayer pattern after oxide etch, (c) nanorods formed after 3 min Cl_2 etch, with SEM inset of the top surface, (d) 300 nm of GaN overgrowth on (c), with SEM inset revealing the apex tipped nanorods, (e) photograph of 2" GaN/AlN/Al_2O_3 wafer coated with a monolayer of silica spheres.

After the GaN top down/bottom up nanorods are formed, InGaN/GaN quantum well/quantum barriers (QW/QBs) are deposited using the growth condition for forming planar QWs on 11-22 semi-polar GaN in the MOCVD reactor (QB growth temperature = 850 ^{0}C and QW growth temperature = 720 ^{0}C). The estimated indium content for the InGaN MQWs grown was 16% according to growth on bulk planar semi-polar GaN. After growth a pointed pyramidal structure is formed at the top of the nanorods, as seen in Figure 2c, with the slanted facets in the 1-101 planes, which form a tilted angle of 62^0 following the same geometry of the GaN nanorod core as seen in SEM analysis of Figure 1d. The ultra-sharp tip can be seen clearly in Figure 2d under transmission electron microcopy (TEM) imaging with the selective area electron diffraction (SAED) revealing the single crystal wurzite structure. The lower growth temperatures of the QW/QBs promote the vertical/0001 growth rate as reported by Hiramatsu et al[48] for GaN micro-

stripes, and as a result any c-plane facet at the top of these rods is shrunk to a sharp tip as seen in Figure 2c.

When a single QW(SQW)/QB of InGaN/GaN is grown on the GaN nanorods, as seen in Figure 2b, the original c-plane although shrinks in diameter, but it does not fully disappear as seen for the MQW nanrods. Reinforcing the idea of increased 0001 growth rate with decreasing growth temperature as stated above. This implies the top diameter and in turn c-plane QW diameter can be controlled easily be manipulating the growth time of the low temperature QB. Initial EDX surface scans of the nanrod tops, Figure 2d and e, indicate a 10 fold increase in In% at the tips compared to the semi-polar sidewalls. The line scan reveals the sharp increase of In% at the top of the nanorods with comparable decrease in Ga content as seen in Figure 2 (e). This result alone indicated that either the In composition of the *c*-plane MQW region was higher than the In composition at the semi polar-plane MQW region or simply the well thickness at the c-plane was far greater in thickness. However through STEM investigation as seen in Figure 5, it was revealed that this sharp peak in In content was due to the much higher growth rate in the c-plane direction for InGaN QWs than at the semi-polar planes also observed by Tu. C.G et al[49].

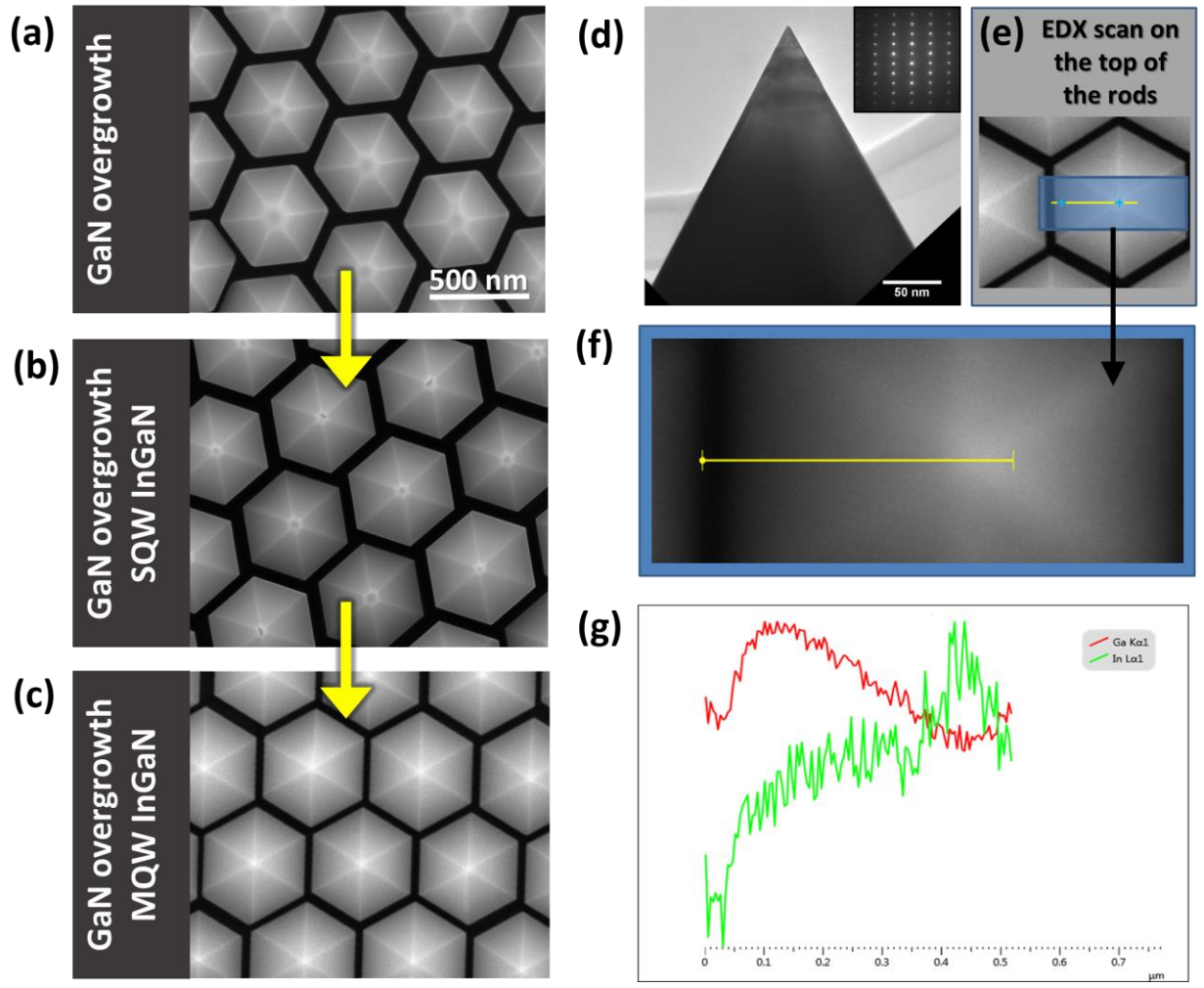

Figure 2 SEM imaging of (a) GaN nanorod overgrowth with truncated apex tips, (b) InGaN/GaN SQW growth on (a) with a smaller c-plane diameter top, (c) InGaN/GaN MQW growth on (a) with a sharp apex tip, (d) TEM of the sharp tip on an individual nanorod with SAED inset showing the wurzite crystal structure with the 0002 growth direction, (e) and (f) EDX line and point scan in SEM mode, (e) spectra from the line scan in (e) and (f).

The initial CL measurements of the close packed nanorod arrays shows the blue emission is coming from the semi-polar planes and not from the nanotips as seen in the emission spectrum highlighted in blue in Figure 3a**.** The tips of each nanorod however emit light in the visible light spectrum >500 nm (highlighted blue region in Figure 3(b)), with no emission in the spectral range coming from the rest of the nanorod. The Correlative CL and SEM of Figure 3b reveal the

drastically different emission wavelength at the tips. This result is in positive agreement with the EDX top surface line scans as seen in Figure 2g. The room temperature photoluminescence analysis in Figure S3 of supporting information of the rods reveals a broad peak in the same wavelength region (i.e. red, yellow, green) as seen for the highlighted red CL spectra of Figure 3b. To investigate the nanoscale optical properties at the nanorod tip and the source of the possible change in composition/well thickness nanorods were exfoliated from the bulk substrate. This was done by using a diamond scribe to scratch off the rods and then dropping onto a lacey poly carbon covered copper grid for scanning transmission electron microscopy (STEM) and hyperspectral CL imaging, Figure 4 and 5.

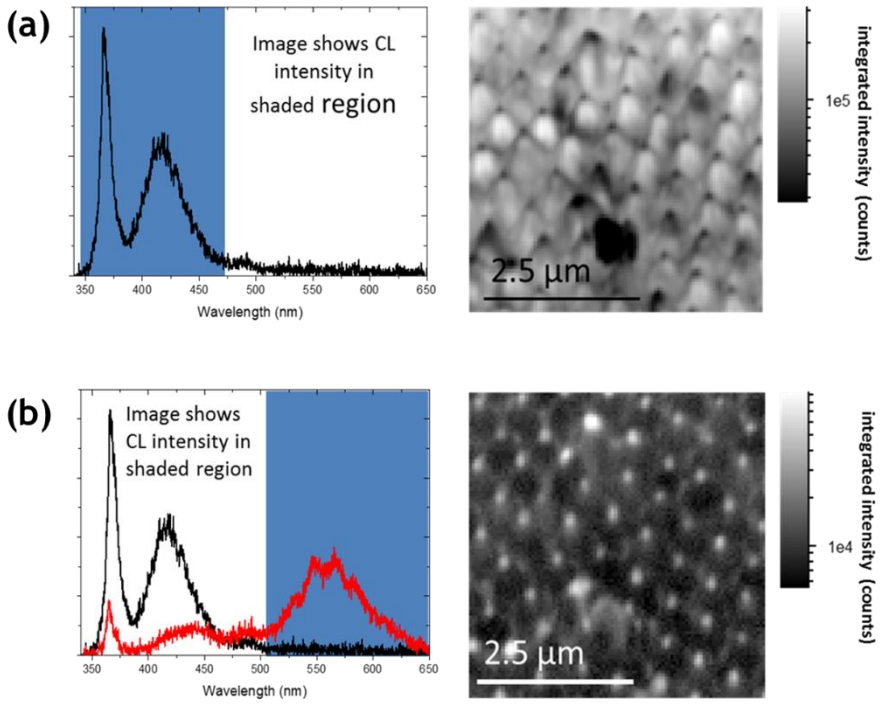

Figure 3 Correlative CL spectra and SEM imaging of the emission: (a) ~350-450 nm spectral range from the semi-polar sidewalls and (b) >500 nm spectral range from only the nanotips.

The real colour representation of the spatially resolved CL emission in Figure 4a, shows the white light from the nanotips. Extracting the spectral information along the line in Figure 4a gives a line spectrum with three distinctive regions of the nanorod of different optical properties; non-polar sidewalls, semi-polar sidewalls and the c-plane tip, as seen in Figure 4b. What is noticeable in the non-polar region is the lack of any yellow luminescence and the small FWHM of the 365 nm peak (Figure 3a), indicating any possible ion beam damage incorporated during the etched nanorod formation was healed. This links well with our previous report for AlN[47] on dislocation reduction of III-N etched nanorods after thermal annealing at MOCVD growth temperatures, that will also be discussed in a detailed report on GaN nanorod annealing in a future publication. The panchromatic intensity map in this UV region (Figure 4c ~365 nm) shows a strong reduction in the luminescence intensity at the point where the top and base of the nanorod meet. The second region at the semi-polar sidewalls is dominated by a broad luminescence band in the blue region (395-465 nm). In the line spectrum there is one main peak with two satellite peaks. It has been suggested by Kusch et al(your APL paper) that these three peaks may be due to some form of optical modes within the rod since the growth conditions for the 5 InGaN MQWs active zone were not varied throughout the growth.

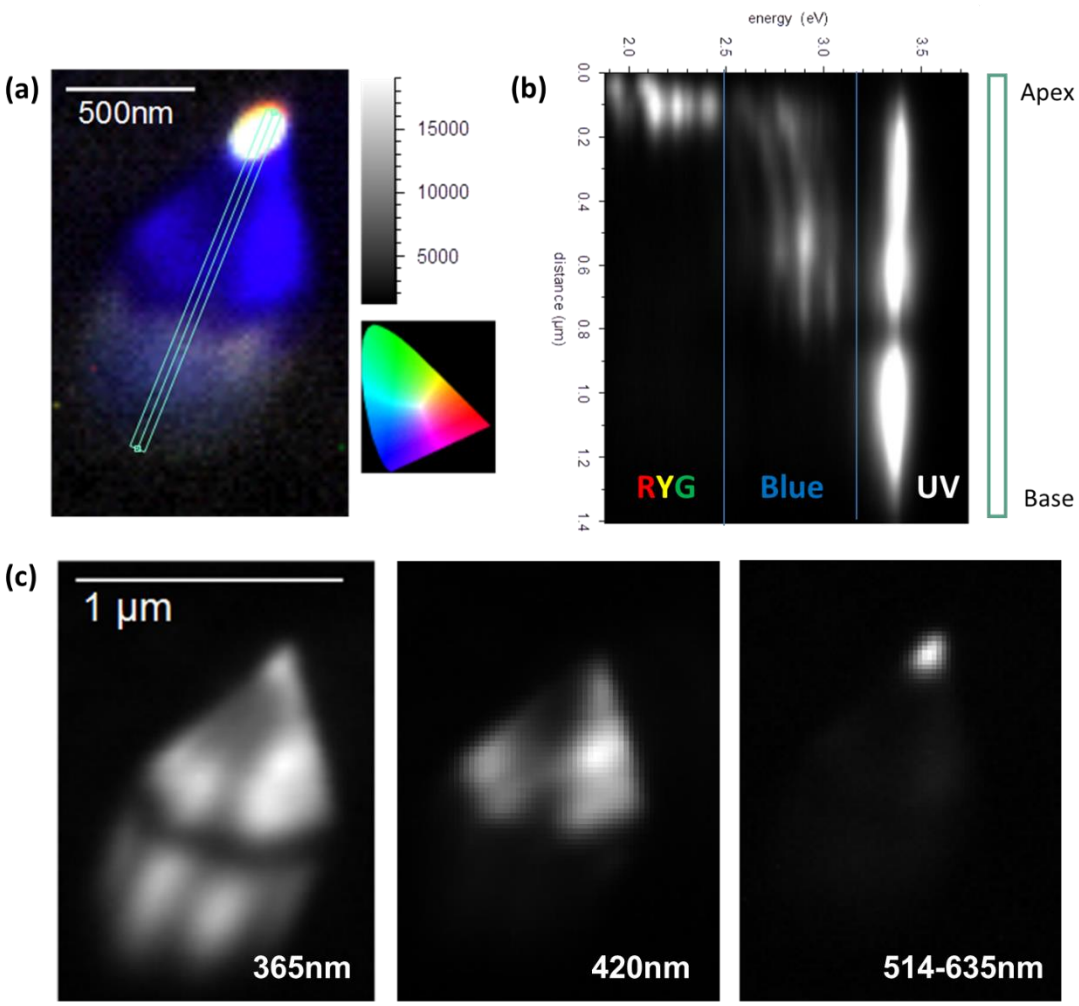

Figure 4 (a) real colour representation of the spatially resolved CL emission, (b) spectral information extracted along the line in (a), (c) spatially resolved CL of the nanorod at increasing wavelength range.

The third light emitting region seen in Figure 4b from the nanotip exhibits a broad luminescence band consisting of multiple peaks covering the visible spectral range from green to red (514-635 nm). These multiple peaks are not believed to be due to optical modes seen in the semi-polar region, as the energy separation between the peaks was in the range 60–185meV and the non-constant energy variation between them that should be near constant for optical modes.

TEM/STEM analysis in Figure 5 of the MQWs support the idea that 5 peaks are not from an optical mode, but instead are from the 5 different MQWs.

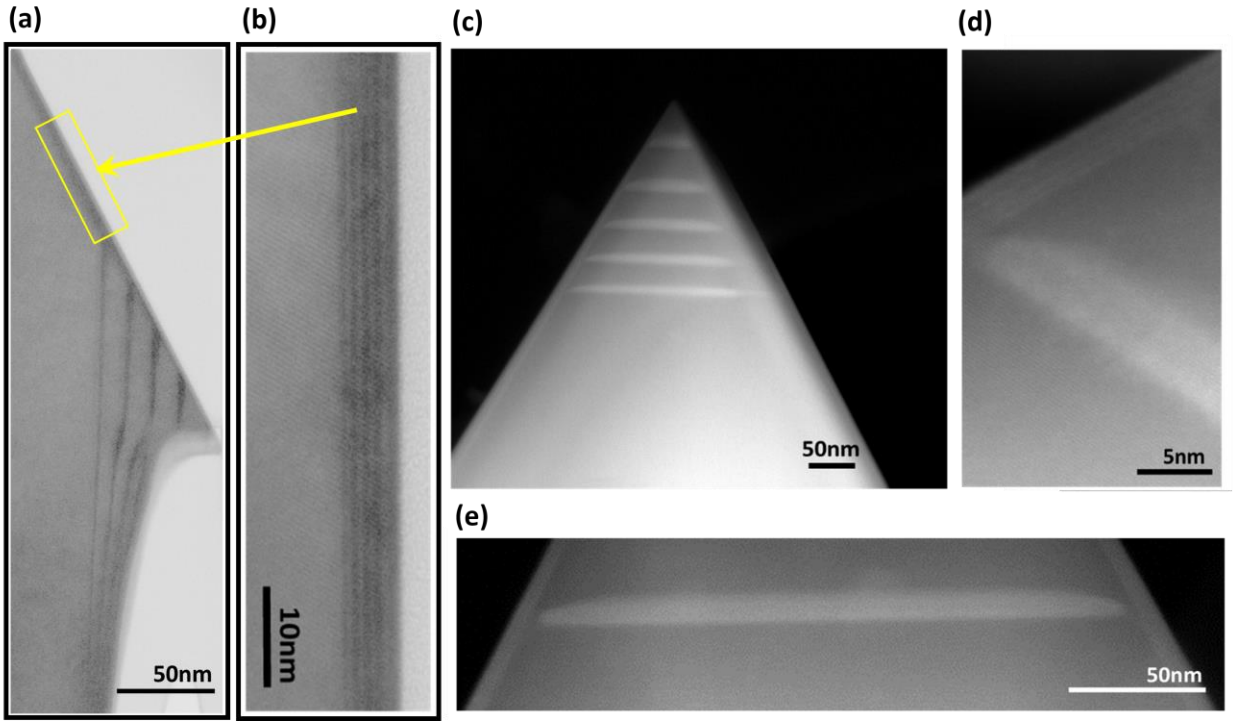

Figure 5 TEM imaging of (a) the semi-/non-polar meeting point revealing the changing in MQW thickness, (b) higher magnification of the 5 X MQW on the semi-polar facets, STEM imaging of (c) the nanorod tip showing the 5 X MQWs increasing in thickness, (d) higher magnification of the meeting point of the 5 X MQWs visible at the semi-polar facet to the first c-plane QW, (e) lower magnification showing the first c-plane QW thickness is greater than the entire 5 X MQW/MQB at the semi-polar plane.

Focused ion beam (FIB) cross sections of the ~550 nm thick nanorods were done to analyze under a 200keV TEM in high resolution as in Figure 5a and b. The stacked bright and dark layers, corresponding to the InGaN QW and QB respectively. Figure 5a shows the edge between the non-polar (1-100) and semi-polar (1-101) planes which reveals slightly thicker QW width, other groups

have explained this by possible different incorporation rates at the edge region due to gas flow i.e. flux shielding of the non-polar plane[50]. However unlike at the thicker QWs on the c-plane where there is a clear individually sharp luminescence peaks (RYG) seen in CL, these meeting points of the non- and semi-polar planes results in nearly no luminescence under CL investigation as seen in Figure 4b and c. This suggests that the irregularity of the QWs at this meeting point as seen in the TEM image of Figure 5a kills the luminescence. The TEM/STEM clearly show significantly large differences in the QW and QB thickness on different growth facets, which may be a result of the anisotropic surface formation energies of GaN crystal planes that are known to influence the diffusion of adatoms.[15, 51-52]

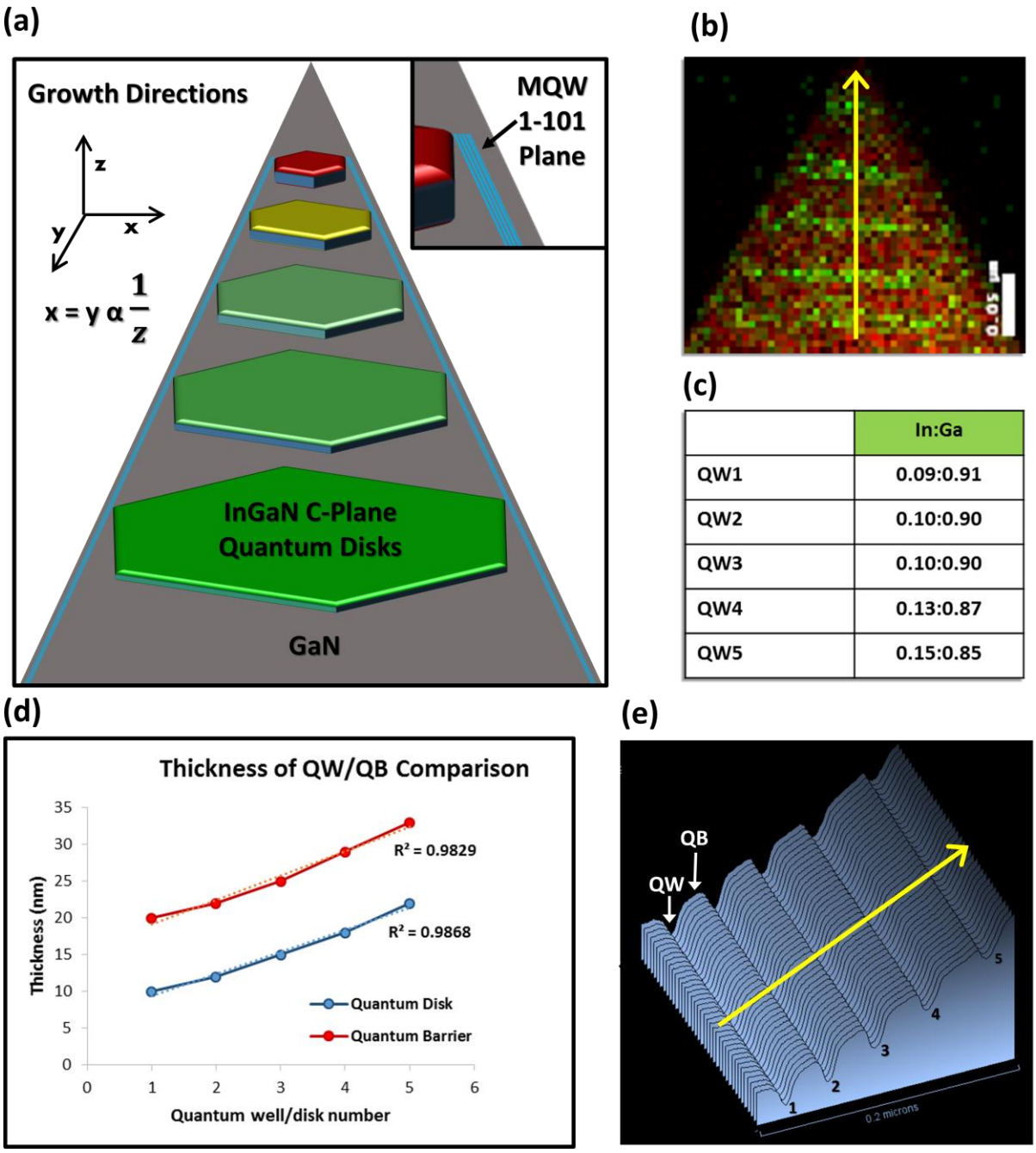

	In:Ga
QW1	0.09:0.91
QW2	0.10:0.90
QW3	0.10:0.90
QW4	0.13:0.87
QW5	0.15:0.85

Figure 6 (a) schematic illustration of the changing thickness for the InGaN wells in all three x,y,z directions at the c-plane, high magnification inset of the constant QW thickness on the semi-polar walls, (b) EDX mapping of the 5 MQWs, (c) table of the In:Ga wt% ratio data at each MQW, (d) graphical plot of the QW/QB thickness data from the line plot along the

yellow line in (b) showing their linear relationship, (e) surface area plot of the 5 X MQW/QBs along the yellow line.

Analysis by surface area spectra done in Image J software illustrates and measures by a 3D model the increasing thickness of the QWs and QBs going up the nanorod. Figure 6e is the 3D spectra along the area indicated with the yellow arrow in the STEM EDX spectra image in Figure 6b, used to extract the lengths of the QWs and QBs. When plotted against each other the increasing QW/QB thickness is seen to have a near linear relationship, Figure 6d. This is a clear indication that the increasing InGaN quantum disc thickness is not majorly due to the higher Indium adatom diffusion length that has been an argument for thicker c-plane active region and higher In % incorporations.[14] Instead the linear relationship with the GaN barrier indicates the change in the quantum disc thickness is thus a direct result in increased growth rate due to the decreasing x/y directional geometry as schematically illustrated in Figure 6a. The 5 luminescence peaks at 516, 534, 551, 577, and 635 nm corresponding to the RYG luminescence clearly distinguishable in Figure 4 and the spectra of supporting information Figure S4. This can be compared to the drastically changing confinement seen in Figure 5 STEM imaging and schematically represented in Figure 6a. The x/y:z ratio of the InGaN QWs change from 18:1 for the first QW to 1.5:1 for the fifth and final QW, numerically portraying the profound shift in directional confinement along the pyramid top.

EDX mapping in STEM high angle annular dark field (HAADF) mode was undertaken at 300 keV to investigate the elemental compositional ratios of the InGaN active regions, Figure 6b. There was an increase in the In% as detailed in the table of Figure 6c from QW1 (9%) to QW5 (15%), however this increase in In% may not be this high in reality when taking into account the possible errors due to the change in interaction volume at the 3D nanotip. Even with this observed increase

in In% the corresponding InGaN alloy ratio is still far too low to emit light in the RYG region of the visible light spectrum, when compared to theoretical calculations and experimental c-plane bulk InGaN QW reports.[53] However Liao. C.H. et al[54] show a much lower In% is needed in InGaN QWs nanorods (15.6-16.8%) for emission >500 nm when the thickness of the wells is increased ~22 nm that is identical to the thickness in the z-direction for our c-plane QWs as seen in Figure 6d. As described above the growth of these very thick InGaN layers occurred only at the c-plane due to an increased growth rate with the decreasing x/y directional geometry, hence the red shift in emission is only seen on the tips of the nanorods and not in the 2 nm thick semi-polar wells.

A possible application for these nanorod geometries would be to concentrate on the growth of single InGaN quantum discs (QDs) on the top of these nanorods for single photon emission. The growth of such QDs has been demonstrated via the Stranski-Krastanov growth mode[55] and other routes.[56] However, these methods do not allow the control of the position and even the size of the nanostructures, which is an essential requirement for applications such as single photon emitters.[57] This growth method of InGaN/GaN nanorods provides a template to allow for wafer-scale position controlled growth of InGaN QD arrays as demonstrated by Juska et al[58] for InGaAs QDs grown in inverted pyramidal arrays.

The results presented in this article prove an emission wavelength >600 nm can be achieved simply by manipulating the directional confinement of InGaN films without increasing the indium of the InGaN MQWs to a high molar fraction. With the stable m-plane nanorod sidewalls formed, the c-plane diameter decreases with the increasing z height following the stablilised 62° semi-polar sidewall along this naturally occurring 1-101 plane. Hence we see an increase in growth rate of both the InGaN MQWs and the GaN barriers without any change in the applied growth parameters within the MOCVD reactor. Therefore along with the experimentally measured low In%, the

possible explanation of compositional pulling often suggested to explain changes in QW thickness on different growth facets and thus shifts in the expected emission wavelength can be eliminated. We conclude that the red shift is most likely due to the increasing QCSE with the thickening InGaN QWs. TEM and STEM show the dislocation and stacking fault free nature of the nanorods with showing the high crystalline quality of these highly dense wafer scale arrays of non-coalesced InGaN/GaN nanorods. The results of this article put forward many possible applications for these nanorods including broad spectrum white lighting sources, but more interestingly possible single photon emitting light sources across the visible light spectrum with controlled positioning of the InGaN QDs on these ordered highly dense nanorod arrays.

AUTHOR INFORMATION

Corresponding Author

* Address correspondence to michele.conroy@pnnl.gov or peter.parbrok@tyndall.ie

Present Addresses

†‡§‖Michele Conroy: Pacific Northwest National Laboratory, 902 Battelle Blvd, Richland, WA 99354, United States.

Acknowledgment. This research was enabled by the Irish Higher Education Authority Programme for Research in Third Level Institutions Cycles 4 and 5 *via* the INSPIRE and TYFFANI projects, and by Science Foundation Ireland (SFI) under Grant no. SFI/10/IN.1/I2993. PJP acknowledges funding from SFI Engineering Professorship scheme (07/EN/E001A) and MC acknowledges PhD research scholarship from INSPIRE. This work was conducted under the

framework of the Irish Government's Programme for Research in Third Level Institutions Cycle 5, National Development Plan 2007–2013 with the assistance of the European Regional Development Fund.Author Contributions

The manuscript was written through contributions of all authors. All authors have given approval to the final version of the manuscript.

Conflict of Interest: The authors declare no competing financial interest.

S*upporting Information Available:*

This material is available free of charge via the Internet at http:// pubs.acs.org.

Detailed SEM investigation of the resulting GaN overgrowth on shorter etched GaN nanorods and the areas of misalignment. PL analysis of the 5 X InGaN MQWs grown on nanorods and planar GaN at the same time. CL spectra of the single InGaN/GaN nanorod on TEM grid.

Acknowledgment. This research was enabled by the Irish Higher Education Authority Programme for Research in Third Level Institutions Cycles 4 and 5 via the INSPIRE and TYFFANI projects, and by Science Foundation Ireland (SFI) under Grant no. SFI/10/IN.1/I2993. PJP acknowledges funding from SFI Engineering Professorship scheme (07/EN/E001A) and MC acknowledges PhD research scholarship from INSPIRE. This work was conducted under the framework of the Irish Government's Programme for Research in Third Level Institutions Cycle 5, National Development Plan 2007–2013 with the assistance of the European Regional Development Fund. RWM and GK acknowledge funding from the Engineering and Physical Sciences Research Council (EPSRC)

(EP/M003132/1) of the UK. We also acknowledge the support of William Jagoe for his illustrations in the article.

REFERENCES

1. Feezell, D. F.; Speck, J. S.; DenBaars, S. P.; Nakamura, S., Semipolar (20-2-1) InGaN/GaN Light-Emitting Diodes for High-Efficiency Solid-State Lighting. *Display Technology, Journal of* **2013,** *9* (4), 190-198.

2. Herrnsdorf, J.; McKendry, J. J. D.; Shuailong, Z.; Enyuan, X.; Ferreira, R.; Massoubre, D.; Zuhdi, A. M.; Henderson, R. K.; Underwood, I.; Watson, S.; Kelly, A. E.; Gu, E.; Dawson, M. D., Active-Matrix GaN Micro Light-Emitting Diode Display With Unprecedented Brightness. *Electron Devices, IEEE Transactions on* **2015,** *62* (6), 1918-1925.

3. Jiang, H. X.; Lin, J. Y., Nitride micro-LEDs and beyond - a decade progress review. *Opt. Express* **2013,** *21* (S3), A475-A484.

4. Wu, J.; Walukiewicz, W.; Yu, K. M.; Ager, J. W.; Haller, E. E.; Lu, H.; Schaff, W. J., Small band gap bowing in In1−xGaxN alloys. *Applied Physics Letters* **2002,** *80* (25), 4741-4743.

5. Kim, J.-H.; Ko, Y.-H.; Cho, J.-H.; Gong, S.-H.; Ko, S.-M.; Cho, Y.-H., Toward highly radiative white light emitting nanostructures: a new approach to dislocation-eliminated GaN/InGaN core-shell nanostructures with a negligible polarization field. *Nanoscale* **2014,** *6* (23), 14213-14220.

6. Detchprohm, T.; Zhu, M.; Li, Y.; Zhao, L.; You, S.; Wetzel, C.; Preble, E. A.; Paskova, T.; Hanser, D., Wavelength-stable cyan and green light emitting diodes on nonpolar m-plane GaN bulk substrates. *Applied Physics Letters* **2010,** *96* (5), 051101.

7. Zhao, W.; Wang, L.; Wang, J.; Hao, Z.; Luo, Y., Theoretical study on critical thicknesses of InGaN grown on (0001) GaN. *Journal of Crystal Growth* **2011,** *327* (1), 202-204.

8. People, R.; Bean, J. C., Calculation of critical layer thickness versus lattice mismatch for GexSi1−x/Si strained-layer heterostructures. *Applied Physics Letters* **1985,** *47* (3), 322-324.

9. Nakajima, K.; Ujihara, T.; Miyashita, S.; Sazaki, G., Effects of misfit dislocations and AlN buffer layer on the GaInN/GaN phase diagram of the growth mode. *Journal of Applied Physics* **2001,** *89* (1), 146-153.

10. Hersee, S. D.; Sun, X.; Wang, X., The controlled growth of GaN nanowires. *Nano Letters* **2006,** *6* (8), 1808-1811.

11. Coltrin, M. E.; Armstrong, A. M.; Brener, I.; Chow, W. W.; Crawford, M. H.; Fischer, A. J.; Kelley, D. F.; Koleske, D. D.; Lauhon, L. J.; Martin, J. E.; Nyman, M.; Schubert, E. F.; Shea-Rohwer, L. E.; Subramania, G.; Tsao, J. Y.; Wang, G. T.; Wierer, J. J.; Wright, J. B., Energy Frontier Research Center for Solid-State Lighting Science: Exploring New Materials Architectures and Light Emission Phenomena. *The Journal of Physical Chemistry C* **2014,** *118* (25), 13330-13345.

12. Guo, W.; Zhang, M.; Banerjee, A.; Bhattacharya, P., Catalyst-free InGaN/GaN nanowire light emitting diodes grown on (001) silicon by molecular beam epitaxy. *Nano letters* **2010,** *10* (9), 3355-3359.

13. Jonathan, J. W., Jr.; Qiming, L.; Daniel, D. K.; Stephen, R. L.; George, T. W., III-nitride core–shell nanowire arrayed solar cells. *Nanotechnology* **2012,** *23* (19), 194007.

14. Yeh, T.-W.; Lin, Y.-T.; Stewart, L. S.; Dapkus, P. D.; Sarkissian, R.; O'Brien, J. D.; Ahn, B.; Nutt, S. R., InGaN/GaN multiple quantum wells grown on nonpolar facets of vertical GaN nanorod arrays. *Nano letters* **2012,** *12* (6), 3257-3262.

15. Hong, Y. J.; Lee, C. H.; Yoon, A.; Kim, M.; Seong, H. K.; Chung, H. J.; Sone, C.; Park, Y. J.; Yi, G. C., Visible-Color-Tunable Light-Emitting Diodes. *Advanced Materials* **2011,** *23* (29), 3284-3288.

16. Yan, R.; Gargas, D.; Yang, P., Nanowire photonics. *Nat Photon* **2009,** *3* (10), 569-576.

17. Ko, Y.-H.; Kim, J.-H.; Gong, S.-H.; Kim, J.; Kim, T.; Cho, Y.-H., Red Emission of InGaN/GaN Double Heterostructures on GaN Nanopyramid Structures. *ACS Photonics* **2015,** *2* (4), 515-520.

18. Wright, J. B.; Liu, S.; Wang, G. T.; Li, Q.; Benz, A.; Koleske, D. D.; Lu, P.; Xu, H.; Lester, L.; Luk, T. S.; Brener, I.; Subramania, G., Multi-Colour Nanowire Photonic Crystal Laser Pixels. *Sci. Rep.* **2013,** *3*.

19. Park, C.; Park, Y.; Im, H.; Kang, T., Optical properties of GaN nanorods grown by molecular-beam epitaxy; dependence on growth time. *Nanotechnology* **2006,** *17* (4), 952.

20. Duan, X.; Lieber, C. M., Laser-assisted Catalytic Growth of Single Crystal GaN Nanowires. *J. Am. Chem. Soc.* **2000,** *122*, 188-189.

21. Kuykendall, T.; Pauzauskie, P.; Lee, S.; Zhang, Y.; Goldberger, J.; Yang, P., Metalorganic Chemical Vapour Deposition Route to GaN Nanowires with Triangular Cross Sections. *Nano Lett.* **2003,** *3*, 1063-1066.

22. Brandt, O.; Fernández-Garrido, S.; Zettler, J. K.; Luna, E.; Jahn, U.; Chèze, C.; Kaganer, V. M., Statistical Analysis of the Shape of One-Dimensional Nanostructures: Determining the Coalescence Degree of Spontaneously Formed GaN Nanowires. *Crystal Growth & Design* **2014,** *14* (5), 2246-2253.

23. Jenichen, B.; Brandt, O.; Pfüller, C.; Dogan, P.; Knelangen, M.; Trampert, A., Macro- and micro-strain in GaN nanowires on Si(111). *Nanotechnology* **2011,** *22* (29), 295714.

24. Fan, S.; Zhao, S.; Liu, X.; Mi, Z., Study on the coalescence of dislocation-free GaN nanowires on Si and SiOx. *Journal of Vacuum Science & Technology B* **2014,** *32* (2), 02C114.

25. Consonni, V.; Knelangen, M.; Jahn, U.; Trampert, A.; Geelhaar, L.; Riechert, H., Effects of nanowire coalescence on their structural and optical properties on a local scale. *Applied Physics Letters* **2009,** *95* (24), 241910.

26. Lefebvre, P.; Fernández-Garrido, S.; Grandal, J.; Ristić, J.; Sánchez-García, M.-A.; Calleja, E., Radiative defects in GaN nanocolumns: Correlation with growth conditions and sample morphology. *Applied Physics Letters* **2011,** *98* (8), 083104.

27. Fernández-Garrido, S.; Kaganer, V. M.; Hauswald, C.; Jenichen, B.; Ramsteiner, M.; Consonni, V.; Geelhaar, L.; Brandt, O., Correlation between the structural and optical properties of spontaneously formed GaN nanowires: a quantitative evaluation of the impact of nanowire coalescence. *Nanotechnology* **2014,** *25* (45), 455702.

28. Yan, L.; Jahangir, S.; Wight, S. A.; Nikoobakht, B.; Bhattacharya, P.; Millunchick, J. M., Structural and Optical Properties of Disc-in-Wire InGaN/GaN LEDs. *Nano Letters* **2015,** *15* (3), 1535-1539.

29. Brandt, O.; Pfüller, C.; Chèze, C.; Geelhaar, L.; Riechert, H., Sub-meV linewidth of excitonic luminescence in single GaN nanowires: Direct evidence for surface excitons. *Physical Review B* **2010,** *81* (4), 045302.

30. Reshchikov, M. A.; Morkoç, H., Luminescence properties of defects in GaN. *Journal of Applied Physics* **2005,** *97* (6), 061301.

31. Kim, J.-H.; Oh, C.-S.; Ko, Y.-H.; Ko, S.-M.; Park, K.-Y.; Jeong, M.; Lee, J. Y.; Cho, Y.-H., Dislocation-Eliminating Chemical Control Method for High-Efficiency GaN-Based Light Emitting Nanostructures. *Crystal Growth & Design* **2012,** *12* (3), 1292-1298.
32. Li, Q.; Wright, J. B.; Chow, W. W.; Luk, T. S.; Brener, I.; Lester, L. F.; Wang, G. T., *Opt. Express* **2012,** *20*, 17873.
33. Li, Q.; Westlake, K. R.; Crawford, M. H.; Lee, S. R.; Koleske, D. D.; Figiel, J. J.; Cross, K. C.; Fathololoumi, S.; Mi, Z.; Wang, G. T., Optical performance of top-down fabricated InGaN/GaN nanorod light emitting diode arrays. *Opt. Express* **2011,** *19* (25), 25528-25534.
34. Wierer, J. J.; Li, Q.; Koleske, D. D.; Lee, S. R.; Wang, G. T., *Nanotechnology* **2012,** *23*, 194007.
35. Lewins, C. J.; Le Boulbar, E. D.; Lis, S. M.; Edwards, P. R.; Martin, R. W.; Shields, P. A.; Allsopp, D. W. E., Strong photonic crystal behavior in regular arrays of core-shell and quantum disc InGaN/GaN nanorod light-emitting diodes. *Journal of Applied Physics* **2014,** *116* (4), 044305.
36. Waag, A.; Wang, X.; Fündling, S.; Ledig, J.; Erenburg, M.; Neumann, R.; Al Suleiman, M.; Merzsch, S.; Wei, J.; Li, S.; Wehmann, H. H.; Bergbauer, W.; Straßburg, M.; Trampert, A.; Jahn, U.; Riechert, H., The nanorod approach: GaN NanoLEDs for solid state lighting. *physica status solidi (c)* **2011,** *8* (7-8), 2296-2301.
37. Conroy, M.; Zubialevich, V. Z.; Li, H.; Petkov, N.; O'Donoghue, S.; Holmes, J. D.; Parbrook, P. J., Ultra-High Density Arrays of Defect Free AlN Nanorods: A 'Space Filling' Approach. *ACS Nano* **2015**.
38. Matsuoka, T.; Yoshimoto, N.; Sasaki, T.; Katsui, A., Wide-gap semiconductor InGaN and InGaAln grown by MOVPE. *Journal of Elec Materi* **1992,** *21* (2), 157-163.
39. Keller, S.; Keller, B. P.; Kapolnek, D.; Abare, A. C.; Masui, H.; Coldren, L. A.; Mishra, U. K.; Den Baars, S. P., Growth and characterization of bulk InGaN films and quantum wells. *Applied Physics Letters* **1996,** *68* (22), 3147-3149.
40. Chichibu, S. F.; Abare, A. C.; Mack, M. P.; Minsky, M. S.; Deguchi, T.; Cohen, D.; Kozodoy, P.; Fleischer, S. B.; Keller, S.; Speck, J. S.; Bowers, J. E.; Hu, E.; Mishra, U. K.; Coldren, L. A.; DenBaars, S. P.; Wada, K.; Sota, T.; Nakamura, S., Optical properties of InGaN quantum wells. *Materials Science and Engineering: B* **1999,** *59* (1–3), 298-306.

41. Benjamin, D.; Nicolas, G.; Cyril, P.; Jean, M., Monolithic White Light Emitting Diodes Based on InGaN/GaN Multiple-Quantum Wells. *Japanese Journal of Applied Physics* **2001,** *40* (9A), L918.

42. Lin, H.-C.; Shu, C.-K.; Ou, J.; Pan, Y.-C.; Chen, W.-K.; Chen, W.-H.; Lee, M.-C., Growth temperature effects on InxGa1−xN films studied by X-ray and photoluminescence. *Journal of Crystal Growth* **1998,** *189–190*, 57-60.

43. Van der Stricht, W.; Moerman, I.; Demeester, P.; Crawley, J. A.; Thrush, E. J., Study of GaN and InGaN films grown by metalorganic chemical vapour deposition. *Journal of Crystal Growth* **1997,** *170* (1–4), 344-348.

44. Yam, F. K.; Hassan, Z., InGaN: An overview of the growth kinetics, physical properties and emission mechanisms. *Superlattices and Microstructures* **2008,** *43* (1), 1-23.

45. Li, H.; Sadler, T. C.; Parbrook, P. J., AlN heteroepitaxy on sapphire by metalorganic vapour phase epitaxy using low temperature nucleation layers. *Journal of Crystal Growth* **2013,** *383* (0), 72-78.

46. Conroy, M. A.; Petkov, N.; Li, H. N.; Sadler, T. C.; Zubialevich, V.; Holmes, J. D.; Parbrook, P. J., Preparation of Substrates Intended for the Growth of Lower Threading Dislocation Densities within Nitride Based UV Multiple Quantum Wells. *ECS Transactions* **2013,** *53* (2), 39-42.

47. Conroy, M.; Zubialevich, V. Z.; Li, H.; Petkov, N.; Holmes, J. D.; Parbrook, P. J., Epitaxial lateral overgrowth of AlN on self-assembled patterned nanorods. *Journal of Materials Chemistry C* **2015,** *3* (2), 431-437.

48. Hiramatsu, K., Epitaxial lateral overgrowth techniques used in group III nitride epitaxy. *Journal of Physics: Condensed Matter* **2001,** *13* (32), 6961.

49. Tu, C.-G.; Su, C.-Y.; Liao, C.-H.; Hsieh, C.; Yao, Y.-F.; Chen, H.-T.; Lin, C.-H.; Chen, H.-S.; Kiang, Y.-W.; Yang, C. C., Regularly-patterned nanorod light-emitting diode arrays grown with metalorganic vapor-phase epitaxy. *Superlattices and Microstructures* **2015,** *83* (0), 329-341.

50. Jung, B. O.; Bae, S.-Y.; Kim, S. Y.; Lee, S.; Lee, J. Y.; Lee, D.-S.; Kato, Y.; Honda, Y.; Amano, H., Highly ordered catalyst-free InGaN/GaN core–shell architecture arrays with expanded active area region. *Nano Energy* **2015,** *11* (0), 294-303.

51. Funato, M.; Kotani, T.; Kondou, T.; Kawakami, Y.; Narukawa, Y.; Mukai, T., KURENAI: Kyoto University Research Information Repository. *Applied physics letters* **2006,** *88* (26), 261920.
52. Y. J. Hong, S. J. A., H.S. Jung, C. H. Lee, G. C. Yi, *Adv. Mater.* **2007,** *19* (4416).
53. Shuji, N.; Masayuki, S.; Naruhito, I.; Shin-ichi, N., High-Brightness InGaN Blue, Green and Yellow Light-Emitting Diodes with Quantum Well Structures. *Japanese Journal of Applied Physics* **1995,** *34* (7A), L797.
54. Liao, C.-H.; Tu, C.-G.; Chang, W.-M.; Su, C.-Y.; Shih, P.-Y.; Chen, H.-T.; Yao, Y.-F.; Hsieh, C.; Chen, H.-S.; Lin, C.-H.; Yu, C.-K.; Kiang, Y.-W.; Yang, C. C., Dependencies of the emission behavior and quantum well structure of a regularly-patterned, InGaN/GaN quantum-well nanorod array on growth condition. *Opt. Express* **2014,** *22* (14), 17303-17319.
55. Kobayashi, Y.; Perez-Solorzano, V.; Off, J.; Kuhn, B.; Gräbeldinger, H.; Schweizer, H.; Scholz, F., Investigations of growth of self-assembled GaInN–GaN islands on SiC substrate by metalorganic vapor phase epitaxy. *Journal of crystal growth* **2002,** *243* (1), 103-107.
56. Ru-Chin, T.; Chun-Ju, T.; Chang-Cheng, C.; Bing-Chi, L.; Ching-En, T.; Te-Chung, W.; Jim, C.; Chien-Ping, L.; Gou-Chung, C., Ultra-High-Density InGaN Quantum Dots Grown by Metalorganic Chemical Vapor Deposition. *Japanese Journal of Applied Physics* **2004,** *43* (2B), L264.
57. Pérez-Solórzano, V.; Gröning, A.; Jetter, M.; Riemann, T.; Christen, J., Near-red emission from site-controlled pyramidal InGaN quantum dots. *Applied Physics Letters* **2005,** *87* (16), 163121.
58. Juska, G.; Dimastrodonato, V.; Mereni, L. O.; Gocalinska, A.; Pelucchi, E., Towards quantum-dot arrays of entangled photon emitters. *Nat Photon* **2013,** *7* (7), 527-531.